Reproducibility of Metabolic Measurements in Malignant Tumors Using FDG PET

Wolfgang A. Weber, Sibylle I. Ziegler, Ralf Thödtmann, Axel-R. Hanauske and Markus Schwaiger

Nuklearmedizinische Klinik and I. Medizinische Klinik, Klinikum Rechts der Isar, Technische Universität München, München, Germany

PET using ^{18}F-fluorodeoxyglucose (FDG) is increasingly applied to monitor the response of malignant tumors to radiotherapy and chemotherapy. The aim of this study was to assess the reproducibility of serial FDG PET measurements to define objective criteria for the evaluation of treatment-induced changes. **Methods:** Sixteen patients participating in phase I studies of novel antineoplastic compounds were examined twice by FDG PET within 10 d while they were receiving no therapy. Standardized uptake values (SUVs), FDG net influx constants (K_i), glucose normalized SUVs (SUV_{gluc}) and influx constants ($K_{i,gluc}$) were determined for 50 separate lesions. The precision of repeated measurements was determined on a lesion-by-lesion and a patient-by-patient basis. **Results:** None of the parameters showed a significant increase or decrease at the two examinations. The differences of repeated measurements were approximately normally distributed for all parameters with an SD of the mean percentage difference of about 10%. The 95% normal ranges for spontaneous fluctuations of SUV, SUV_{gluc}, K_i and $K_{i,gluc}$ were determined to be ±0.91, ±1.14, ±0.52 mL/100 g/min and ±0.64 mL/100 g/min, respectively. Analysis on a lesion-by-lesion basis yielded similar results. **Conclusion:** FDG PET provides several highly reproducible quantitative parameters of tumor glucose metabolism. Changes of a parameter that are outside the 95% normal range determined in this study may be used to define a metabolic response to therapy.

Key Words: PET; fluorodeoxyglucose; therapy monitoring

J Nucl Med 1999; 40:1771–1777

The potential of PET using the glucose analog ^{18}F-fluorodeoxyglucose (FDG) for imaging of malignant tumors has been widely documented in the literature (*1*). Currently, FDG PET is used mainly for tumor detection and staging. For these applications, a qualitative image interpretation has been found to be sufficient in most cases (*2–4*). However, PET also allows quantitative measurements of activity concentrations within the body. Because of the simple metabolic pathway of FDG, these activity concentrations can be used to estimate the glucose utilization of malignant tumors. In several small studies, FDG PET measurements have been applied to monitor the response of malignant tumors to therapy (*5–12*). These studies showed that a reduced number of viable cells or reduced metabolism of damaged cells is associated with a decrease in FDG uptake. Therefore, changes in FDG uptake after chemotherapy and radiotherapy may provide a new marker for tumor response (*5–12*).

However, knowledge of the degree of reproducibility of FDG PET measurements is mandatory for reliable detection of changes over time. Before FDG PET can be applied for therapy monitoring in clinical practice and research, the accuracy of the measuring technique and the spontaneous variability of the biologic signal have to be determined.

Thus, the aim of this study was to assess the reproducibility of serial FDG PET measurements in malignant tumors. A group of patients with advanced tumor stages who participated in phase I studies were examined twice by FDG PET within 10 d while they were receiving no therapy. A three-dimensional delineation of the tumors was performed, and the reproducibility of commonly applied parameters of glucose metabolism was determined. The data were then used to calculate normal ranges for random statistical fluctuations of the parameters. These normal ranges provide objective criteria to determine whether an observed decrease of a parameter after therapy represents a true change in glucose metabolism or can be explained by statistical fluctuation. Thus, the normal ranges allow definition of a metabolic response in individual patients. Furthermore, the normal ranges may be applied to determine the number of patients that must be included in a therapy monitoring study to detect therapy-induced changes in glucose metabolism with a certain statistical power.

MATERIALS AND METHODS

Patient Population

The study population consisted of 16 patients (11 men, 5 women; age 57 ± 9 y) who participated in phase I studies at this institution. Before the first course of chemotherapy, patients were examined by FDG PET twice within 10 d (mean 3 ± 3 d). No chemotherapy, radiotherapy or surgical treatment had been performed at least 4 wk before the first PET scan. Fifty separate tumor lesions were evaluated (8 primary tumors, 22 lung metastases, 12 lymph node metastases and 8 liver metastases) in the 16 patients.

Received Sep. 10, 1998; revision accepted Apr. 9, 1999.

For correspondence or reprints contact: Wolfgang A. Weber, MD, Nuklearmedizinische Klinik, Klinikum Rechts der Isar, Ismaningerstr. 22, 81675 München, Germany.

Patient characteristics, histologic diagnosis and localization of the lesions are summarized in Table 1.

Details of the study were explained to the patients, and written informed consent was obtained. The study protocol was reviewed and approved by the Ethics Committee of the Technische Universität München.

Imaging Procedure

Imaging was performed using a whole-body PET scanner (ECAT EXACT; CTI/Siemens, Inc., Knoxville, TN). This imaging device consists of 24 rings of bismuth germaneate detectors that yield 47 transverse slices, 3.4 mm apart.

^{18}F was produced with a self-shielded 11-MeV cyclotron (RDS 112; CTI/Siemens, Inc.) by the acceleration of protons onto an ^{18}O water target. FDG was produced with a standard technique modified from the synthesis reported by Hamacher et al. (*13*).

Patients fasted at least 4 h before PET imaging to minimize glucose utilization of normal tissue and to ensure standardized glucose metabolism in all patients. The serum glucose level was measured before the PET examination using blood glucose reagent strips and photometric measurement (Glucometer II and Glucostix; Bayer Diagnostics, Munich, Germany). After positioning the patient in the scanner, a transmission measurement with ^{68}Ge rod sources was performed for 15 min to yield approximately 4 million counts per slice.

After transmission measurement, a bolus of approximately 370 MBq FDG was injected through an intravenous catheter, and a dynamic acquisition sequence was begun. The mode of data acquisition was identical for both scans and consisted of six 10-s frames, eight 30-s frames, five 1-min frames, six 5-min frames and three 10-min frames (total acquisition time 70 min).

Emission data corrected for random coincidences, dead time and attenuation were reconstructed by filtered backprojection (Hanning filter with cutoff frequency 0.4 cycle per bin). The matrix size was 128 × 128 pixels with a size of 4.0 × 4.0 mm. The image pixel counts were calibrated to activity concentrations (becquerels per milliliter) and decay corrected using the time of tracer injection as a reference. The resulting in-plane image resolution of transaxial images was approximately 8-mm full width at half maximum (FWHM), with an axial resolution of approximately 5-mm FWHM.

TABLE 1
Characteristics of Patients in Study

Patient no.	Age (y)	Sex	No. of lesions	Localization of lesions	Diagnosis
1	56	M	6	Lung	NSCLC
2	65	M	1	Pleura	Mesothelioma
3	58	M	1	Pleura	Mesothelioma
4	64	F	1	Lung	NSCLC
5	55	M	6	Lung	Metastatic esophageal cancer
6	73	F	1	Mediastinum	Lymph node metastases of NSCLC
7	59	M	4	Cervix and mediastinum	Lymph node metastases of NSCLC
8	58	F	1	Lung	Metastatic vulvar carcinoma
9	53	F	3	Pelvis	Recurrent rectal cancer (lymph node metastases)
10	68	M	1	Pleura	Mesothelioma
11	49	M	2	Mediastinum	NSCLC
12	50	M	4	Liver	Metastatic rectal cancer
13	37	F	8	Mediastinum and lung	High-grade non-Hodgkin's lymphoma
14	60	M	2	Mediastinum	Metastatic renal cancer
15	45	M	5	Lung	Metastatic adenoid cystic cancer
16	56	M	4	Liver	Metastatic rectal cancer

NSCLC = non-small cell lung cancer.

Data Analysis

For definition of regions of interest (ROIs) and data analysis, computer programs were developed in the Interactive Data Language (IDL; Research Systems, Inc., Boulder, CO) using the Clinical Application Programming Package (CAPP; CTI/Siemens, Inc.). Standardized uptake values (SUVs), FDG net influx constants (K_i), glucose normalized SUVs (SUV_{gluc}) and net influx constants ($K_{i,gluc}$) were calculated.

Region-of-Interest Definition

For definition of tumor volumes, the last frame of the dynamic study (60–70 min after injection) was used. Loosely fitting ROIs covering the whole tumor volume were manually placed around the lesions in consecutive slices. Tumor volumes were then defined using a cutoff value of 50% of the maximum FDG concentration within this volume. The second to fourth frames of the dynamic study were used to define the blood ROIs needed for calculation of the input function. Blood time-activity curves were generated from ROIs placed in the left ventricle (11 patients) or the aorta (5 patients). For the left ventricular cavity, circular ROIs with a diameter of 1.2 cm were placed in two consecutive slices in the left ventricle. For the aorta, square 2 × 2 pixel ROIs were placed in the aorta in eight consecutive slices (*14*). Average counts derived from the blood ROIs were used to calculate the input function.

Calculation of Parameters

SUVs were calculated in the last frame of the dynamic study (60–70 min after injection) using the formula: SUV = measured activity concentration (Bq/g) × body weight (g)/injected activity (Bq).

SUV_{gluc} were calculated by multiplying the SUV with the measured blood glucose concentration and dividing by 100 mg/100 mL. To evaluate the influence of the time point of measurement on the SUV, additional SUVs were also calculated at 40 and 50 min after injection

The Patlak-Gjedde graphic method was used to determine K_i (*15*). The starting point of the analysis was 10 min after injection. Metabolic rates for FDG ($K_{i,gluc}$) were calculated by multiplying K_i with the blood glucose concentration and dividing by 100 mg/100 mL.

Statistical Analysis

For each tumor lesion, the difference between the measurements of a parameter at the two time points, d, was calculated. The distribution of d was analyzed using probability plots. In this plot, a normally distributed sample is represented by a straight line. Deviations from normality result in curved plots. Furthermore, deviation from normality was tested using the Kolmogorov-

Smirnov test, and the mean skewness of the distribution of d was calculated. The skewness of a dataset corresponds to the mean minus the median divided by the SD. This parameter indicates whether positive or negative deviations of d from the mean are more pronounced (*16*). The Kolmogorov-Smirnov test determines the probability that differences between the observed distribution and the normal distribution are associated with random sampling fluctuation. Thus, a low probability of the Kolmogorov-Smirnov test provides evidence that the observed data are not normally distributed (*16*).

After confirmation of an approximately normal distribution, the mean and SD of d were calculated. Two times the SD of d was then used to define the normal range of spontaneous changes in a parameter. To estimate the precision of the calculated normal ranges, 95% confidence intervals of the SD of d were calculated using the chi-square distribution (*16*).

For comparison of the reproducibility of the different parameters, mean relative differences, D (mean of d divided by the global mean of a parameter) and intraclass correlation coefficients (ICs) were determined. The IC describes the correlation between two measurements of a parameter. If the two measurements give identical results, the IC is one. Random or systematic differences between the two measurements decrease the value of the IC. Differences in the variance of D for the various parameters were tested using the F test and Bartlet's test (*16*). The F test compares the SD of two normally distributed datasets. Bartlet's test is a generalization of the F test that allows comparison of more than two data sets.

Analysis of the reproducibility of the various parameters was performed on a patient-by-patient and a lesion-by-lesion basis. For the patient-by-patient analysis, the lesion with the highest FDG uptake 60–70 min after injection in the first study was used.

Bartlet's test was also used to determine whether there were significant differences in the variance of the parameters in patients with different numbers of lesions. To accomplish this, patients were grouped into four groups: group 1, 1–2 lesions; group 2, 3–4 lesions; group 3, 4–6 lesions; and group 4, 7 or more lesions.

The reproducibility of blood curves was assessed by comparing the differences in areas under the time-activity curve corrected for injected doses in studies 1 and 2.

A paired two-sided *t* test was applied to test for differences of the means of the various parameters at the two scans. To assess the influence of tumor size on the reproducibility of a parameter, the absolute value of the differences at the two measurements, |d|, was plotted against the tumor volume, and linear regression analysis was applied. The same method was used to determine whether there is a correlation between |d| and the value of the measured parameter. All statistical tests were performed at the 5% level of significance.

RESULTS

Tables 2 and 3 show the mean ± SD for each of the measured parameters from studies 1 and 2 on a patient-by-patient and a lesion-by-lesion basis. None of the parameters showed a significant increase or decrease between the two scans. Both SUV and the influx constant, K_i, have an IC of 0.99. The SD of the mean percentage difference was approximately 9% for both parameters. The mean tumor volume estimated from the number of pixels included in the 50% isocontours used for ROI definition was 17 ± 24 mL (range 0.8–111 mL). For spherical lesions this corresponds to a mean diameter of 3.2 ± 3.6 cm (range 1.2–6.0 cm). The mean percentage difference for repeated determinations of the tumor volume was 3% ± 18%.

Mean blood glucose levels at the two PET scans were 102 ± 12 (range 81–123 mg/100 mL) and 101 ± 12 mg/100 mL (range 75–116 mg/100 mL) ($P = 0.8$). SUV_{gluc} and $K_{i,gluc}$ showed approximately the same variability as the uncorrected values ($P > 0.4$ by F test for SD of mean percentage differences). The area under the blood time-activity curve was also highly reproducible with an SD of the mean percentage difference of 8% and an IC of 0.99. Figure 1 is a graphic comparison of the mean percentage differences of the various parameters on a lesion-by-lesion basis.

TABLE 2
Calculated Parameters of Glucose Metabolism and Their Reproducibility: Patient-by-Patient Analysis of Data

Parameter	Study 1	Study 2	IC	d	D	95% normal range for change	95% confidence interval for normal range
AUC_{blood} (mL × min)	8.05 ± 3.45 (4.44–16.55)	8.05 ± 3.35 (4.53–16.44)	0.99	0.003 ± 0.60 (−1.52–1.11)	0.0% ± 7.5% (−19%–14%)	±1.20	1.10–1.31
SUV	5.50 ± 2.58 (1.25–10.30)	5.51 ± 2.79 (1.34–10.80)	0.99	0.017 ± 0.46 (−0.85–0.72)	0.34% ± 9.1% (−17%–14%)	±0.91	0.69–1.45
SUV_{gluc}	5.59 ± 2.58 (1.22–11.23)	5.56 ± 2.90 (1.31–12.57)	0.98	−0.03 ± 0.57 (−1.04–1.33)	0.69% ± 12% (−22%–27%)	±1.14	0.86–1.86
K_i (mL/100 g/min)	3.37 ± 2.07 (0.62–8.41)	3.41 ± 2.18 (0.64–8.84)	0.99	−0.18 ± 0.88 (−1.42–1.58)	1.2% ± 8.3% (−10%–13%)	±0.52	0.39–0.85
$K_{i,gluc}$ (mL/100 g/min)	3.51 ± 2.35 (0.61–9.54)	3.47 ± 2.34 (0.62–9.04)	0.99	−0.04 ± 0.32 (−0.49–0.85)	−1.13% ± 10% (−16%–27%)	±0.64	0.48–1.04

IC = intraclass correlation coefficient; d = mean difference of parameter in study 1 and study 2; D = mean percentage difference of parameter in study 1 and study 2 (d divided by global mean of parameter in study 1 and study 2); AUC = area under blood time-activity curve; SUV = standardized uptake value; SUV_{gluc} = glucose normalized SUV; K_i = influx constant; $K_{i,gluc}$ = glucose normalized influx constant.

Lesion with highest ^{18}F-fluorodeoxyglucose uptake in study 1 was chosen as index lesion for measuring reproducibility.

TABLE 3
Calculated Parameters of Glucose Metabolism and Their Reproducibility: Lesion-by-Lesion Analysis of Data

Parameter	Study 1	Study 2	IC	d	D	95% normal range for change	95% confidence interval for normal range
SUV	5.02 ± 2.30 (1.25–10.30)	5.05 ± 2.36 (1.34–10.80)	0.99	0.06 ± 0.45 (−0.85–1.05)	0.5% ± 8.6% (−17%–14%)	±0.90	0.76–1.13
SUV_{gluc}	4.90 ± 2.16 (1.20–11.20)	4.83 ± 2.16 (1.31–12.56)	0.98	−0.10 ± 0.43 (−1.05–1.34)	−1.0% ± 8.6% (−22%–24%)	±0.86	0.73–1.09
K_i (mL/100 g/min)	3.17 ± 1.74 (0.62–8.40)	3.18 ± 1.81 (0.64–8.84)	0.99	0.01 ± 0.27 (−0.74–0.54)	0.4% ± 9.0% (−23%–17%)	±0.54	0.46–0.68
$K_{i,gluc}$ (mL/100 g/min)	3.21 ± 2.01 (0.61–9.53)	3.12 ± 1.94 (0.63–9.54)	0.98	−0.03 ± 0.35 (−1.05–0.85)	−1.0% ± 10.0% (−33%–27%)	±0.70	0.59–0.88

IC = intraclass correlation coefficient; d = mean difference of parameter in study 1 and study 2; D = mean percentage difference of parameter in study 1 and study 2 (d divided by global mean of parameter in study 1 and study 2); SUV = standardized uptake value; SUV_{gluc} = glucose normalized SUV; K_i = influx constant; $K_{i,gluc}$ = glucose normalized influx constant.
Lesion with highest ^{18}F-fluorodeoxyglucose uptake in study 1 was chosen as index lesion for measuring reproducibility.

The estimated mean and SDs of D and d obtained from the lesion-by-lesion analysis and the patient-by-patient analysis were almost identical. Bartlet's test showed no significant differences in the SD of d for any of the parameters between the groups of patients with different numbers of lesions ($P > 0.7$). Both results indicate that the main source of variability is the variability in the measurement of individual lesions. Therefore, the following description considers only the results of the lesion-by-lesion analysis, which allows more precise estimates of the statistical parameters.

Kolmogorov-Smirnov testing revealed no significant deviation of d from normality for any of the parameters. Figure 2 shows the probability plot of d for K_i as an example. The SD of d was not influenced by the absolute value of the parameter ($r = 0.98$, $P < 0.01$ by linear regression analysis). The volume of the lesion had no influence on SUV and SUV_{gluc} ($P > 0.3$ by linear regression analysis). For K_i and $K_{i,gluc}$, there was a trend for increased variability with decreasing volume of the lesion; however, this was not statistically significant ($P = 0.06$). The skewness of the distribution of d was low for all parameters (range −0.21 to 0.11).

These results indicate that two times the SD of d is a valid estimate for the normal range of absolute changes in a parameter. The last two columns of Table 2 give these normal ranges for the various parameters with their 95% confidence intervals.

For therapy monitoring, relative changes in glucose metabolism are more important than the absolute values. Because the normal range for absolute changes in a parameter remains constant, the normal range for relative changes widens with decreasing initial value. Therefore, normal ranges of relative changes in a parameter were calculated depending on the mean value of the parameter in both studies. Figure 3 shows these normal ranges for K_i with the corresponding 95% confidence intervals. The values for

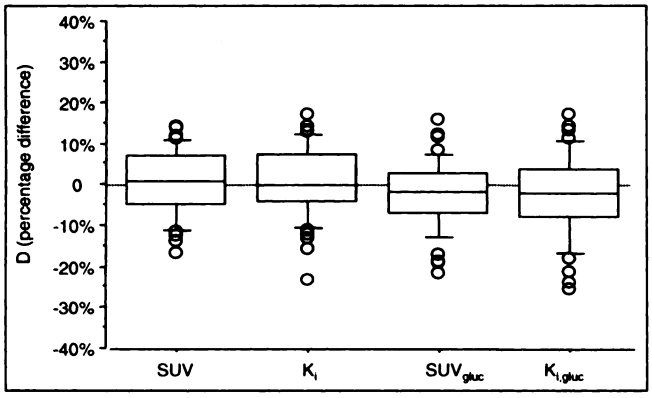

FIGURE 1. Graphic comparison of mean percentage difference, D, for various parameters analyzed on lesion-by-lesion basis. Boxes represent values between 25th and 75th percentiles; horizontal bars (inside boxes) indicate median; vertical bars (above and below boxes) represent values at 10th and 90th percentiles. SUV = standardized uptake value; K_i = influx constant; SUV_{gluc} = glucose normalized SUV; $K_{i,gluc}$ = glucose normalized influx constant.

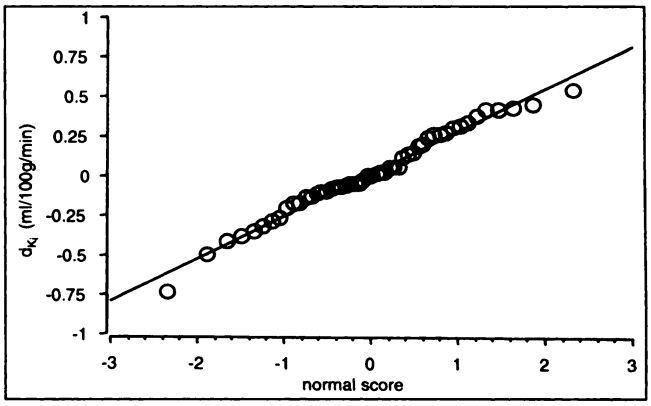

FIGURE 2. Probability plot of difference between measurements of a parameter at two time points, d, for influx constant, K_i (= d_{K_i}). Distribution of d shows no systematic deviation from normality.

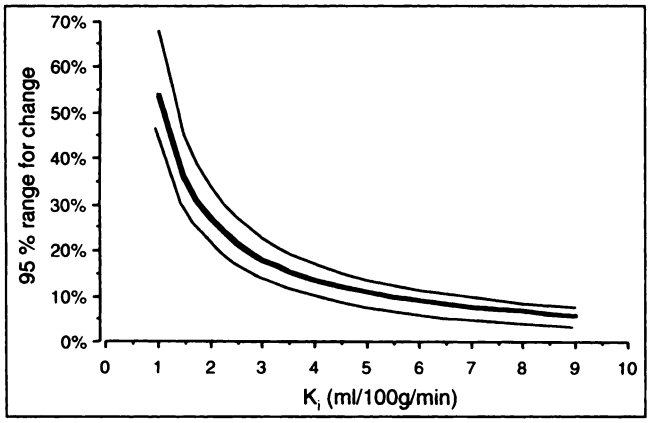

FIGURE 3. Normal ranges for relative changes of influx constant, Ki, with corresponding 95% confidence intervals (thin lines) depending on initial value of K_i.

SUV, SUV_{gluc} and $K_{i,gluc}$ are very similar and therefore are not shown in the graph.

Between 40 and 60 min, there was a significant increase in the SUV of the tumor lesion. The mean SUV for studies 1 and 2 increased by 16% from 4.5 ± 2.3 to 5.1 ± 2.3 (P = 0.02). However, the reproducibility of the SUV was not dependent on the time point of measurement. The ICs for SUVs determined 40, 50 and 60 min after injection were 0.98, 0.99 and 0.99, respectively, and the mean percentage differences were 0.02% ± 0.50%, 0.03% ± 0.47% and 0.06% ± 0.45%, respectively.

DISCUSSION

This study shows that in patients entering clinical trials for new cytotoxic drug regimens, serial FDG PET measurements of tumor metabolism can be performed with high accuracy. For a typical lesion, changes of a parameter of more than 20% are outside the 95% range for spontaneous fluctuations and therefore can be considered to reflect true changes in glucose metabolism of the tumor mass. However, the 95% range for relative change depends on the initial value of a parameter. Therefore, as indicated in Figure 3, different ranges should be used for lesions with different initial FDG uptake.

To our knowledge, the reproducibility of FDG PET in malignant tumors has been analyzed in only 10 patients with lung cancer (*17*). The small number of lesions in that study did not allow determination of the distribution of spontaneous changes and calculation of normal ranges. Furthermore, only large untreated primary tumors with a mean diameter of approximately 5 cm were studied. Thus, the patient population was not representative of patients entering clinical trials for the evaluation of new chemotherapeutic drugs.

Relatively few studies have assessed the reproducibility of tumor volume determinations by CT in patients. A recent study found a mean coefficient of variation (COV) of 11% for the volume determination of liver metastases (*18*). The mean volume of these tumors was 45 mL. For laryngeal tumors (mean tumor volume 5 mL), considerably higher COVs ranging between 16.5% and 113% have been reported (*19*). For CT measurements of brain tumors, the volume change required to be statistically significant has been calculated to be 20% (*20*).

Metabolic imaging using FDG PET for determination of tumor response has several advantages compared with conventional imaging techniques. The high contrast of FDG PET scans allows an automated three-dimensional delineation of tumor tissue by simple thresholding techniques. In contrast, volumetric analysis of CT and MRI studies requires a time-consuming tracing of tumor contours on contiguous slices by an experienced observer. The ill-defined borders of a lesion often make accurate determination of tumor extension impossible. Accordingly, interobserver variability has consistently been found to be a major source of variability in volume determinations (*18,19*). In addition, CT and MRI often may not distinguish between viable tumor cell mass, necrosis and scar tissue, whereas FDG accumulation occurs only in the presence of viable cells. Therefore, FDG uptake may be more closely related to the viable tumor mass than volume determined by morphologic imaging modalities. Furthermore, changes in glucose metabolism may precede structural changes that eventually lead to a decrease in tumor volume. Therefore, FDG PET may allow earlier detection or exclusion of antitumor activity of new cytotoxic drugs in clinical phase I and II trials.

Several parameters have been used to quantify tumor glucose metabolism by FDG PET. SUVs are confined to the measurement of radioactivity concentrations at a fixed time point. Two advantages of SUVs are that they are computationally very simple and require considerably less scanner time than dynamic studies. A major disadvantage of SUVs in therapy monitoring is the dependency on the time of measurement. In this study we found a 16% increase between 40 and 60 min after injection. This finding is in accordance with previous studies that reported a steady increase of SUV up to 90 min after injection (*21*). Therefore, for therapy control studies, it is mandatory that lesions be measured at exactly the same time point at baseline and follow-up.

Determination of K_i requires dynamic data acquisition and determination of a blood time-activity curve. This study shows that, despite this more complex acquisition protocol, K_i values can be measured with the same reproducibility as SUVs. The main advantage of K_i values is that they take into account changes in the whole-body distribution of FDG. However, patient movement during acquisition can cause considerable errors, especially in small lesions. We tried to minimize this effect in this study by performing a three-dimensional delineation of the tumors to maximize the number of pixels that were included in the analysis. Nevertheless, we observed a trend for less reproducible values of K_i in small lesions.

The reproducibility of FDG PET for therapy monitoring is related to numerous factors that can be classified into two groups: first, differences in the metabolic state of the patient

that lead to a different whole-body distribution of FDG; and second, spontaneous variability of glucose consumption within the tumor mass.

The FDG accumulation in a tissue is proportional to the area under the plasma time-activity curve of FDG. This parameter determines the amount of tracer that is available for the tumor and reflects changes in the whole-body distribution of FDG. The low variability of the area under the blood time-activity curve in this study indicates that changes in the whole-body distribution were not a major factor affecting the reproducibility of measurements.

However, this may be different in patients who are imaged during a therapy that changes the distribution volumes of FDG. Hyperglycemia decreases the blood clearance of FDG, and hyperinsulinemia increases tracer uptake by insulin-sensitive tissues such as muscles (*22–24*). Thus, any form of treatment that interferes with glucose metabolism of normal organs (e.g., corticosteroids) will also indirectly affect FDG uptake by tumor tissue. Under these circumstances, measurement of the input function and calculation of influx constants may be preferable to the use of SUVs.

In addition to changes of the whole-body distribution of FDG, hyperglycemia decreases the accumulation of FDG in tumor tissue by competitive inhibition of transport and phosphorylation. Blood glucose normalization of FDG PET parameters has been proposed to compensate for this effect. This method has improved the differentiation of benign from malignant tumors by SUVs (*25*). In this study, we did not observe an improved reproducibility of glucose normalized parameters (SUV_{gluc} and $K_{i,gluc}$); this finding is probably associated with the minimal changes in blood glucose level at scans 1 and 2. In principle, measurement of blood glucose introduces an additional source of error in the calculation of a parameter. The COV for repeated measurements of blood glucose by reagent strips is approximately 5% (*26*). Thus, the benefits of glucose normalization may be offset by errors in blood glucose measurement when there are only small differences in blood glucose levels at the time of the two PET scans. However, for patients who display more marked changes of their blood glucose levels during treatment, blood glucose normalization may be helpful (*24*). More sophisticated laboratory techniques for measurement of blood glucose levels may be used to further improve the reproducibility of FDG PET studies in these patients. Furthermore, fasting periods longer than the 4-h interval used in this study may be required to achieve a stable metabolic state in patients with impaired glucose tolerance (*27*).

Spontaneous changes in the glucose metabolism of a tumor mass cannot be measured directly in patients. However, previous experimental and clinical studies indicate that FDG uptake within a tumor mass may be influenced by numerous factors. Tumor cell density, hypoxia, cellular proliferation and tumor grading have been shown to affect FDG uptake (*28–30*). Furthermore, non-neoplastic elements of a tumor mass such as macrophages and granulation tissue may accumulate considerable amounts of FDG (*31*). Thus, the source of the FDG signal measured by a clinical PET study is complex and may be influenced by factors other than the number of viable tumor cells. Accordingly, cytotoxic therapy may affect FDG uptake within the tumor mass by mechanisms other than reduction of viable tumor cells. For example, radiotherapy has been shown to induce inflammatory reactions that may increase FDG uptake (*32*). Thus, the clinical usefulness of FDG PET for therapy monitoring has to be determined individually for different forms of therapy and different tumor types.

Nevertheless, this study indicates that FDG PET meets three important requisites for successful therapy monitoring. First, the PET technique allows highly reproducible serial measurements of several parameters of tumor glucose metabolism. Second, the measurements can be performed using a relatively simple protocol. Third, spontaneous short-term fluctuations in glucose metabolism of the tumor mass appear to be low.

When these encouraging results are used as a basis for planning and analysis of therapy monitoring studies, several limitations should be noted.

The normal ranges determined in this study are derived from a group of patients with stable fasting blood glucose levels. Therefore, the ranges should be used cautiously when there are markedly different blood glucose levels at the time of baseline and follow-up PET scans. SUVs will be less reliable under these circumstances.

The reproducibility of FDG PET measurements may be affected by lesion size. In fact, we observed a trend for higher variability of K_i in smaller lesions. Therefore, the normal ranges determined in this study should be applied only for lesions with similar sizes. However, most patients undergoing neo-adjuvant or palliative chemotherapy or radiotherapy present with advanced disease. In most of these patients there will be one or more lesions with sizes similar to those analyzed in this study.

The normal ranges of this study apply only to measurements that are repeated within a few days. After a longer interval, changes in tumor size or spontaneous necrosis in rapidly growing tumors may induce considerably larger changes in FDG PET measurements. However, effective chemotherapy can cause a marked reduction in tumor glucose metabolism within 7 d (*33*). Thus, short-term measurements of glucose metabolism for therapy monitoring appear feasible and may allow early differentiation of responding and nonresponding tumors.

The patient population of this study was heterogeneous, and only a limited number of tumor types were included. Furthermore, most lesions were located in the thorax. The low level of background activity in this area facilitates tumor delineation in FDG PET studies. The higher and more variable level of background activity in other parts of the body may lead to a higher variability of FDG PET measurements. Thus, future studies are warranted that evaluate the

normal ranges defined in this study for other tumor types and other localization of lesions.

CONCLUSION

This study shows that FDG PET provides several highly reproducible quantitative parameters of tumor glucose metabolism, which underline the great potential of FDG PET for response monitoring. The normal ranges for spontaneous fluctuations of a parameter determined in this study allow definition of criteria for a metabolic tumor response in individual patients. These ranges also form the basis for planning clinical trials that are aimed at detecting therapy-induced changes in glucose metabolism with a given statistical power.

ACKNOWLEDGMENTS

The authors gratefully acknowledge the effort of the cyclotron and radiochemistry staff, the excellent technical support by the PET technologists and the editorial help of Jodi Neverve in preparation of the manuscript.

REFERENCES

1. Rigo P, Paulus P, Kaschten B, et al. Oncological applications of positron emission tomography with fluorine-18 fluorodeoxyglucose. *Eur J Nucl Med.* 1996;23:1641–1674.
2. Avril N, Dose J, Janicke F, et al. Assessment of axillary lymph node involvement in breast cancer patients with positron emission tomography using radiolabeled 2-(fluorine-18)-fluoro-2-deoxy-D-glucose. *J Natl Cancer Inst.* 1996;88:1204–1209.
3. Avril N, Dose J, Janicke F, et al. Metabolic characterization of breast tumors with positron emission tomography using F-18 fluorodeoxyglucose. *J Clin Oncol.* 1996;14:1848–1857.
4. Lowe VJ, Hoffman JM, DeLong DM, Patz EF, Coleman RE. Semiquantitative and visual analysis of FDG-PET images in pulmonary abnormalities. *J Nucl Med.* 1994;35:1771–1776.
5. Hoekstra OS, Ossenkoppele GJ, Golding R, et al. Early treatment response in malignant lymphoma, as determined by planar fluorine-18-fluorodeoxyglucose scintigraphy. *J Nucl Med.* 1993;34:1706–1710.
6. Haberkorn U, Strauss LG, Dimitrakopoulou A, et al. Fluorodeoxyglucose imaging of advanced head and neck cancer after chemotherapy. *J Nucl Med.* 1993;34:12–17.
7. Minn H, Soini I. [^{18}F]fluorodeoxyglucose scintigraphy in diagnosis and follow up of treatment in advanced breast cancer. *Eur J Nucl Med.* 1989;15:61–66.
8. Torizuka T, Tamaki N, Inokuma T, et al. Value of fluorine-18-FDG-PET to monitor hepatocellular carcinoma after interventional therapy. *J Nucl Med.* 1994;35:1965–1969.
9. Rege SD, Chaiken L, Hoh CK, et al. Change induced by radiation therapy in FDG uptake in normal and malignant structures of the head and neck: quantitation with PET. *Radiology.* 1993;189:807–812.
10. Jansson T, Westlin JE, Ahlstrom H, Lilja A, Langstrom B, Bergh J. Positron emission tomography studies in patients with locally advanced and/or metastatic breast cancer: a method for early therapy evaluation? *J Clin Oncol.* 1995;13:1470–1477.
11. Patz EF Jr, Lowe VJ, Hoffman JM, Paine SS, Harris LK, Goodman PC. Persistent or recurrent bronchogenic carcinoma: detection with PET and 2-[F-18]-2-deoxy-D-glucose. *Radiology.* 1994;191:379–382.
12. Wahl RL, Zasadny K, Helvie M, Hutchins GD, Weber B, Cody R. Metabolic monitoring of breast cancer chemohormonotherapy using positron emission tomography: initial evaluation. *J Clin Oncol.* 1993;11:2101–2111.
13. Hamacher K, Coenen HH, Stocklin G. Efficient stereospecific synthesis of no-carrier-added 2-[^{18}F]-fluoro-2-deoxy-D-glucose using aminopolyether supported nucleophilic substitution. *J Nucl Med.* 1986;27:235–238.
14. Ohtake T, Kosaka N, Watanabe T, et al. Noninvasive method to obtain input function for measuring tissue glucose utilization of thoracic and abdominal organs. *J Nucl Med.* 1991;32:1432–1438.
15. Patlak CS, Blasberg RG, Fenstermacher JD. Graphical evaluation of blood-to-brain transfer constants from multiple-time uptake data. *J Cereb Blood Flow Metab.* 1983;3:1–7.
16. Armitage P, Berry G. *Statistical Methods in Medical Research.* 3rd ed. Oxford, England: Blackwell Scientific; 1994.
17. Minn H, Zasadny KR, Quint LE, Wahl RL. Lung cancer: reproducibility of quantitative measurements for evaluating 2-[F-18]-fluoro-2-deoxy-D-glucose uptake at PET. *Radiology.* 1995;196:167–173.
18. Van Hoe L, Van Cutsem E, Vergote I, et al. Size quantification of liver metastases in patients undergoing cancer treatment: reproducibility of one-, two-, and three-dimensional measurements determined with spiral CT. *Radiology.* 1997;202:671–675.
19. Hermans R, Feron M, Bellon E, Dupont P, Van den Bogaert W, Baert AL. Laryngeal tumor volume measurements determined with CT: a study on intra- and interobserver variability. *Int J Radiat Oncol Biol Phys.* 1998;40:553–557.
20. Mahaley MS Jr, Gillespie GY, Hammett R. Computerized tomography brain scan tumor volume determinations. Sensitivity as an objective criterion of response to therapy. *J Neurosurg.* 1990;72:872–878.
21. Hamberg LM, Hunter GJ, Alpert NM, Choi NC, Babich JW, Fischman AJ. The dose uptake ratio as an index of glucose metabolism: useful parameter or oversimplification? *J Nucl Med.* 1994;35:1308–1312.
22. Minn H, Nuutila P, Lindholm P, et al. In vivo effects of insulin on tumor and skeletal muscle glucose metabolism in patients with lymphoma. *Cancer.* 1994;73:1490–1498.
23. Lindholm P, Minn H, Leskinen Kallio S, Bergman J, Ruotsalainen U, Joensuu H. Influence of the blood glucose concentration on FDG uptake in cancer: a PET study. *J Nucl Med.* 1993;34:1–6.
24. Langen KJ, Braun U, Rota Kops E, et al. The influence of plasma glucose levels on fluorine-18-fluorodeoxyglucose uptake in bronchial carcinomas. *J Nucl Med.* 1993;34:355–359.
25. Avril N, Bense S, Ziegler SI, et al. FDG PET in breast cancer: quantitative image analysis. *J Nucl Med.* 1997;38:1186–1191.
26. Devreese K, Leroux-Roels G. Laboratory assessment of five glucose meters designed for self-monitoring of blood glucose concentration. *Eur J Clin Chem Clin Biochem.* 1993;31:829–837.
27. Diederichs CG, Staib L, Glatting G, Beger HG, Reske SN. FDG PET: elevated plasma glucose reduces both uptake and detection rate of pancreatic malignancies. *J Nucl Med.* 1998;39:1030–1033.
28. Clavo AC, Brown RS, Wahl RL. Fluorodeoxyglucose uptake in human cancer cell lines is increased by hypoxia. *J Nucl Med.* 1995;36:1625–1632.
29. Minn H, Joensuu H, Ahonen A, Klemi P. Fluorodeoxyglucose imaging: a method to assess the proliferative activity of human cancer in vivo—comparison with DNA flow cytometry in head and neck tumors. *Cancer.* 1988;61:1776–1781.
30. Haberkorn U, Strauss LG, Reisser C, et al. Glucose uptake, perfusion, and cell proliferation in head and neck tumors: relation of positron emission tomography to flow cytometry. *J Nucl Med.* 1991;32:1548–1555.
31. Kubota R, Yamada S, Kubota K, Ishiwata K, Tamahashi N, Ido T. Intratumoral distribution of fluorine-18-fluorodeoxyglucose in vivo: high accumulation in macrophages and granulation tissues studied by microautoradiography. *J Nucl Med.* 1992;33:1972–1980.
32. Haberkorn U, Strauss LG, Dimitrakopoulou A, et al. PET studies of fluorodeoxyglucose metabolism in patients with recurrent colorectal tumors receiving radiotherapy. *J Nucl Med.* 1991;32:1485–1490.
33. Romer W, Hanauske AR, Ziegler S, et al. Positron emission tomography in non-Hodgkin's lymphoma: assessment of chemotherapy with fluorodeoxyglucose. *Blood.* 1998;91:4464–4471.